Chemico-Biological Interactions 181 (2009) 236–242

Contents lists available at ScienceDirect

Chemico-Biological Interactions

journal homepage: www.elsevier.com/locate/chembioint

Estrogen-related receptor α (ERRα) inverse agonist XCT-790 induces cell death in chemotherapeutic resistant cancer cells

Feng Wu[a,1], Junjian Wang[a,1], Yanfei Wang[a], Tim-Tak Kwok[b], Siu-Kai Kong[b], Chiwai Wong[a,*]

[a] Guangzhou Institute of Biomedicine and Health, Chinese Academy of Sciences, Guangzhou Science City 510663, China
[b] Department of Biochemistry, Chinese University of Hong Kong, Shatin, Hong Kong

ARTICLE INFO

Article history:
Received 23 March 2009
Received in revised form 6 May 2009
Accepted 8 May 2009
Available online 21 May 2009

Keywords:
Multi-drug resistance (MDR)
Estrogen-related receptor alpha (ERRα)
Reactive oxygen species (ROS)

ABSTRACT

Estrogen-related receptor alpha (ERRα) is primarily thought to regulate energy homeostasis through interacting with peroxisome proliferator-activated receptor γ coactivator-1α and -1β (PGC-1α and -1β). They coordinately control the transcription of genes in the oxidative phosphorylation pathway. In addition to its role in energy metabolism, ERRα has also been implicated as a prognostic marker for breast, ovarian, colon and prostate cancers. In this study, we found that an ERRα inverse agonist XCT-790 induced cell death in HepG2 hepatocarcinoma and its multi-drug resistance (MDR) sub-line R-HepG2. Using a dye Mitotracker Green which stains mitochondrion independent of mitochondrial membrane potential ($\Delta\Psi_m$), we found that XCT-790 dose-dependently decreased mitochondrial mass. Intriguingly, XCT-790 increased $\Delta\Psi_m$ upon short term treatment but decreased $\Delta\Psi_m$ upon longer term treatment. The changes of $\Delta\Psi_m$ in turn promoted the production of reactive oxygen species (ROS) and led to ROS-mediated caspases 3/7, 8, 9 activation and cell death. Importantly, we established that an anti-oxidative compound Mn(III) Tetra(4-benzoic acid) porphyrin chloride (MnTBAP) blocked the caspases activities and cell death increased by XCT-790 treatment. Finally, we found that XCT-790 synergized with paclitaxel to induce cell death in multi-drug resistance sub-line R-HepG2. Our results provide a conceptual framework for further developing chemotherapeutics based on suppressing ERRα activity.

1. Introduction

Estrogen-related receptors alpha, beta and gamma (ERRα, ERRβ, and ERRγ) are orphan nuclear hormone receptors that display constitutively active transcriptional activities [1]. ERRα is primarily thought to regulate energy homeostasis through interacting with peroxisome proliferator-activated receptor γ coactivator-1α and -1β (PGC-1α and -1β). They coordinately control the transcription of genes in the oxidative phosphorylation pathway [2]. In addition to its role in energy metabolism, ERRα has also been implicated as a prognostic marker for breast, ovarian, colon and prostate cancers [3–7]. Importantly, over-expression of ERRα is linked to poor clinical outcome for breast cancer [3,7], suggesting that ERRα may represent a novel target for cancer treatment [8]. Indeed, suppressing the expression of ERRα by RNA interference inhibited the growth of estrogen receptor negative breast cancer cells [9]. In addition, a synthetic chemical XCT-790 designed and demonstrated to function as a specific inverse agonist of ERRα synergized with estrogen receptor antagonist to inhibit the growth of estrogen receptor positive breast cancer cells [10,11].

Chemotherapeutics like doxorubicin and paclitaxel (Taxol) have been widely used in the cancer treatments. Unfortunately, many cancer cells develop multi-drug resistance (MDR) during prolonged systemic treatments [12]. Particularly, aberrant expressions or activities of ATP-binding cassette (ABC) transporter families including subfamily B member 1 (ABCB1), also known as P-glycoprotein 1 (P-GP) or multi-drug resistance 1 (MDR1), and sub-family G member 5 (ABCG5) are associated with MDR [13,14]. These ATP-dependent plasma membrane transporters exclude a variety of structurally and functionally unrelated anti-cancer drugs to the extra-cellular environment, effectively lowering the intra-cellular drug concentration.

Previously, we and others had established a MDR1 over-expressing cell line R-HepG2 to be used as an *in vitro* model system to screen for novel chemotherapeutics that would potentially overcome MDR [15]. In this study, we found that ERRα inverse agonist XCT-790 would induce cell death in HepG2 and its MDR sub-line R-HepG2, suggesting that XCT-790 may be further developed as a novel chemotherapeutic agent.

* Corresponding author. Tel.: +86 20 3229 0256; fax: +86 20 3229 0606.
E-mail address: wong_chiwai@gibh.ac.cn (C. Wong).
[1] These authors contribute equally to this study.

0009-2797/$ – see front matter © 2009 Elsevier Ireland Ltd. All rights reserved.
doi:10.1016/j.cbi.2009.05.008

2. Materials and methods

2.1. Cell culture and reagents

MES-SA, MES-SA/DX5, and HepG2 cells were obtained from American Type Culture Collection. R-HepG2 cells were obtained from the Chinese University of Hong Kong. MES-SA and MES-SA/DX5 cells were cultured in MEM (Gibco) medium with 10% FBS (Hyclone) and 100 U/ml penicillin–streptomycin (Gibco). HepG2 and R-HepG2 cells were cultured in RPMI 1640 (Gibco) medium with 10% FBS and 100 U/ml penicillin–streptomycin. R-HepG2 cells were maintained in culture medium with 1.2 μM doxorubicin to keep their MDR properties. All cells were cultured in a humidified atmosphere containing 5% CO_2 at 37 °C. XCT-790 was synthesized and purified as described [10]. Mn(III) Tetra(4-benzoic acid) porphyrin chloride (MnTBAP) was purchased from Calbiochem. Caspase inhibitor Z-VAD-FMK was purchased from Promega. All other chemicals were purchased from Sigma.

2.2. Cell viability assay

Cells were seeded in 96-well plates at a density of 2000 cells per well and treated with different concentrations of XCT-790 for indicated time with dimethyl sulfoxide (DMSO) as vehicle control. Cell viability was determined by using CellTiter-Glo Luminescent Cell Viability Assay kit (Promega) and recorded by a Veritas™ Microplate luminometer (Turner Biosystems) following technical manuals. Each treatment was performed in triplicate wells per experiment.

2.3. Western blot analysis

Cells were lysed using RIPA reagent (Shanghai Shenneng) according to the manufacturer's protocol and protein extracts were analyzed by 10% SDS-PAGE and blotted onto PVDF membrane. Membranes were incubated with rabbit anti-human PGC-1α antibody (Cell Signaling Technology), rabbit anti-human ERRα antibody generated in house, or mouse anti-human β-actin antibody (Boster) followed by horseradish peroxidase-conjugated secondary antibody (Amersham) and developed with ECL reagent (Amersham).

2.4. Mitochondrial mass determination

Mitotracker green FM (Invitrogen) was used to determine the mitochondrial mass in cells. Briefly, cells were incubated in serum free medium (pre-warmed to 37 °C) with 150 nM Mitotracker Green FM for 20 min in the dark. After staining, cells were washed twice with cold phosphate-buffered saline (PBS) and suspended in 200 μl PBS. Subsequently, cells were analyzed on a flow cytometer (FAC-SCalibur, BD Biosciences) with excitation at 490 nm and emission at 516 nm. Data were processed by using the CellQuest program (BD Biosciences).

2.5. Mitochondrial DNA copy determination

Total DNA was isolated and the amount of mitochondrial DNA (mitochondrial cytochrome c oxidase subunit II) relative to nuclear genomic DNA (β-actin) was determined by Real-time PCR with SYBR green kit (Takara) in MJ Real-time PCR system.

2.6. Mitochondrial membrane potential determination

Mitochondrial membrane potential ($\Delta\Psi_m$) was analyzed by a fluorescent dye JC-1 (Beyotime Jiangsu China). JC-1 is capable of selectively entering mitochondria where it forms monomers and emits green fluorescence when $\Delta\Psi_m$ is relatively low. At high $\Delta\Psi_m$, JC-1 aggregates and gives a red fluorescence. Assays were initiated by incubating HepG2 and R-HepG2 cells with JC-1 for 20 min at 37 °C in the dark and the fluorescence of separated cells was detected with a flow cytometer (FAC-SCalibur, BD Biosciences). Data were processed by using the CellQuest program (BD Biosciences).

2.7. Reactive oxidant species (ROS) determination

The determination of reactive oxidant species (ROS) level was based on the oxidation of 2,7-dichlorodihydrofluorescin (DCFH) (Beyotime Jiangsu China) by peroxide, as previously described [16]. In brief, HepG2 and R-HepG2 cells were washed and incubated with DCFH for 20 min at 37 °C in the dark. Cells were then washed twice and harvested in PBS. The fluorescence of 2, 7-dichlorofluorescein (DCF) was detected with a flow cytometer (FAC-SCalibur, BD Biosciences) with excitation at 488 nm and emission at 530 nm. Data were processed by using the CellQuest program (BD Biosciences).

2.8. Caspase activity determination

The activities of caspases were measured with Caspase-Glo Assay kit (Promega). Briefly, cells were seeded in 96-well plates at a density of 2000 cells/well. After treatment, cells were mixed to shake with 100 μl Caspase-Glo reagent for 2 min and incubated at room temperature for 30 min. Subsequently, luminescence of each sample was recorded by using a Veritas™ Microplate luminometer (Turner Biosystems) following the technical manual. Each treatment was performed in triplicate wells per experiment.

2.9. Assessment of apoptosis

Annexin V-PE apoptosis detection kit I (BD Biosciences) was used to quantitatively determine the percentage of cells within a population that are actively undergoing apoptosis. Briefly, cells were washed twice with cold PBS and resuspended in 1× Binding Buffer at a concentration of 1×10^6 cells/ml, then 100 μl of the solution (1×10^5 cells) were transferred to a 5 ml culture tube, and 5 μl of Annexin V-PE and 5 μl of 7-amino-actinomycin D (7-AAD) were added. Subsequently, cells were gently mixed and incubated for 15 min at room temperature (25 °C) in the dark. Finally cells were suspended in 400 μl PBS for analysis using a flow cytometer (FAC-SCalibur, BD Biosciences) and data were processed by using the CellQuest program (BD Biosciences).

2.10. RNA isolation and quantitative real-time PCR

Total RNA was extracted by Trizol reagent (Invitrogen). The first-strand cDNA was generated with random primer by reverse transcription kits (Invitrogen). Real-time PCR reactions were performed with SYBR green kit (Takara) in MJ Real-time PCR system. Relative gene expression was normalized to 18S rRNA level. Sequences of primers and reaction conditions are available upon request.

2.11. Statistical analysis

Data are presented as mean ± SD and analyzed with unpaired Student's *t*-test. Asterisks indicate significant differences ($^{*}P < 0.05$, $^{**}P < 0.01$, $^{***}P < 0.001$).

3. Results

3.1. Sensitivities of cancer cells to doxorubicin and XCT-790

The sensitivities of human hepatocarcinoma cell line HepG2 and its MDR subline R-HepG2 to doxorubicin and ERRα inverse ago-

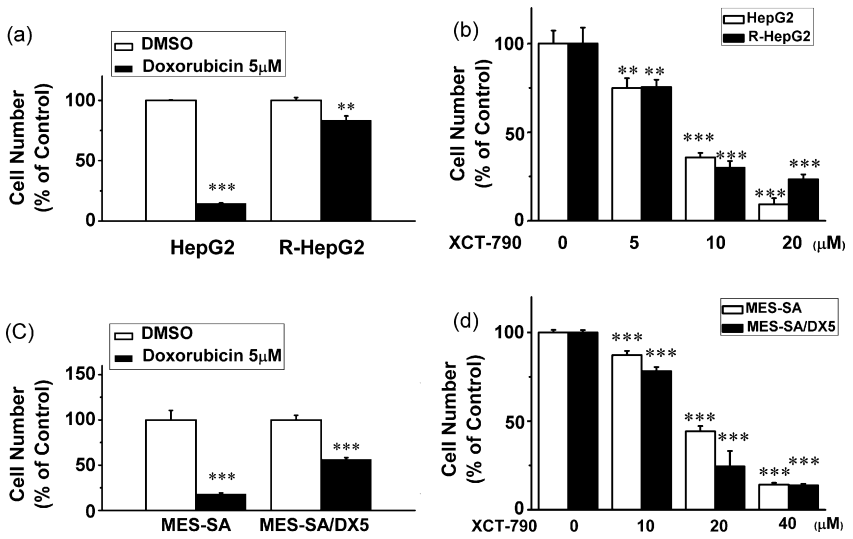

Fig. 1. Sensitivities of cancer cells to doxorubicin and XCT-790. (a) HepG2 and R-HepG2 cells were treated with DMSO or 5 μM doxorubicin (Dox) for 48 h. Cell viabilities were measured as in materials and methods with the DMSO treatment set at 100%; (b) HepG2 and R-HepG2 cells were treated with DMSO or different doses of XCT-790 for 48 h; (c) MES-SA and MES-SA/DX5 cells were treated with DMSO or 5 μM doxorubicin (Dox) for 72 h; (d) MES-SA and MES-SA/DX5 cells were treated with DMSO or different doses of XCT-790 for 72 h; (b–d) Cells were measured as in (a). Data were expressed as mean ± SD of three independent experiments. Asterisks indicate significant differences ($^{*}P<0.05$, $^{**}P<0.01$, $^{***}P<0.001$).

nist XCT-790 were measured after drug treatments for 48 h by cell viability assays. As previously shown, R-HepG2 was resistant to 5 μM of doxorubicin compared to its parental line HepG2 (Fig. 1a). On the other hand, the viabilities of both HepG2 and R-HepG2 were reduced by XCT-790 in dose-dependent manners (Fig. 1b). In addition, we compared the sensitivities of another MDR cell line MES-SA/DX5 [17] and its parental line MES-SA to doxorubicin and XCT-790. We found that MES-SA/DX5 was moderately resistant to doxorubicin compared to MES-SA (Fig. 1c) while XCT-790 reduced the viabilities of both cell lines (Fig. 1d). These results suggested that XCT-790 may have a potential to overcome MDR *in vitro*.

3.2. Effects of XCT-790 on ERRα/PGC-1α expressions and mitochondrial mass

Since R-HepG2 showed the highest level of resistance to doxorubicin but yet sensitive to XCT-790 treatment, we chose R-HepG2 and its parental line HepG2 to further investigate into the mechanism of growth suppression. In view of the crucial role of mitochondria in regulating cell growth and that ERRα regulates mitochondrial biogenesis with coactivator PGC-1α [18,19], we first addressed if XCT-790 altered the expression levels of these proteins. Consistent with a previous report [11], XCT-790 reduced the protein levels of

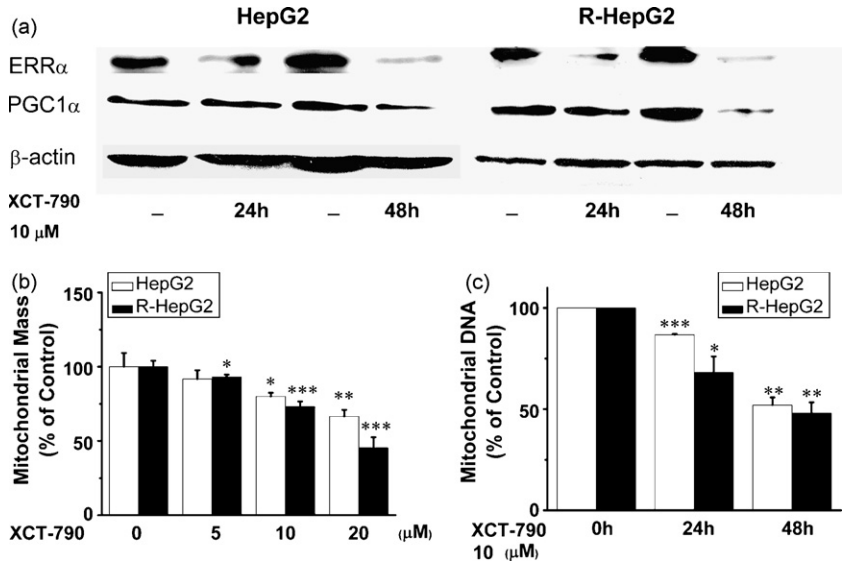

Fig. 2. Effects of XCT-790 on ERRα/PGC-1α expressions and mitochondrial mass. (a) Relative protein expression levels of ERRα and PGC-1α were determined by Western blots. HepG2 and R-HepG2 cells were treated with DMSO or 10 μM XCT-790 for the time indicated. ERRα, PGC-1α expression levels were normalized to β-actin as an internal control. The results are representative of three independent experiments. (b) Mitochondrial mass was determined by flow cytometry with Mitotracker Green FM. HepG2 and R-HepG2 cells were treated with DMSO or XCT-790 at the concentrations indicated for 24 h. The relative mass of DMSO-treated cells was set at 100%. (c) HepG2 and R-HepG2 cells were treated with DMSO or 10 μM XCT-790 for the time indicated. The amount of mitochondrial DNA (mitochondrial cytochrome c oxidase subunit II) relative to nuclear genomic DNA (β-actin) was determined by Real-time PCR. Values are shown as mean ± SD of three independent experiments. Asterisks indicate significant differences ($^{*}P<0.05$, $^{**}P<0.01$, $^{***}P<0.001$).

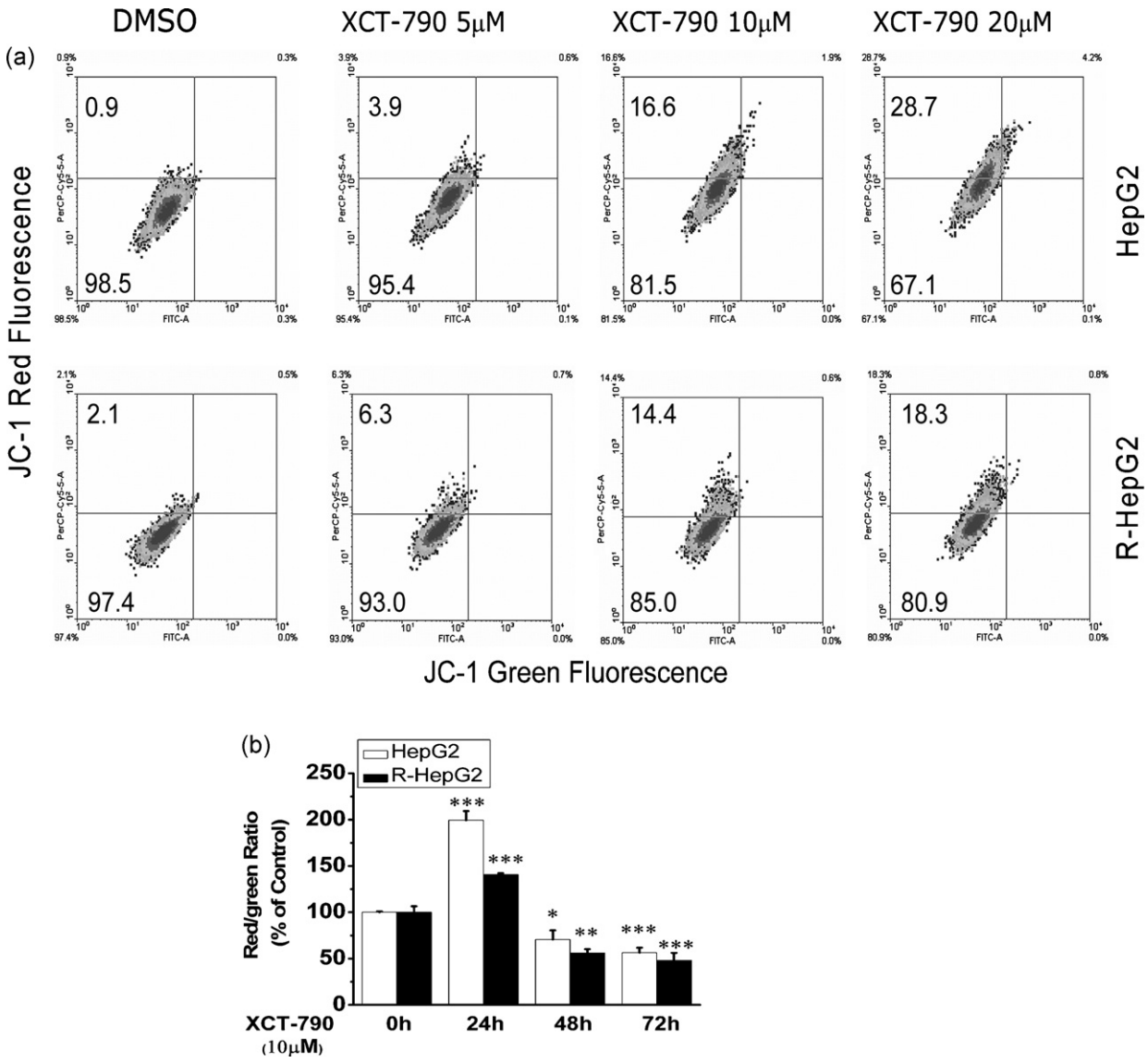

Fig. 3. Effects of XCT-790 on mitochondrial membrane potential. Mitochondrial membrane potential ($\Delta\Psi_m$) was determined by flow cytometry with JC-1. HepG2 and R-HepG2 cells were treated with DMSO or XCT-790 at the concentrations indicated for 24 h. Cells with more red fluorescence mean higher membrane potential. The numbers at the corners represent the percentage of cells in the corresponding quadrants. Results are representative of three independent experiments. (b) The red to green fluorescence ratios upon 10 μM XCT-790 treatments for 24, 48, and 72 h were calculated in HepG2 and R-HepG2 cells. Values are shown as mean ± SD of three independent experiments. Asterisks indicate significant differences ($^{*}P < 0.05$, $^{**}P < 0.01$, $^{***}P < 0.001$).

ERRα in these cell lines after 24 h and maintained these reduced levels after 48 h (Fig. 2a). Importantly, XCT-790 treatment also led to reduced levels of PGC-1α in both HepG2 and R-HepG2 after 48 h (Fig. 2a). We then measured the effect of XCT-790 on mitochondrial mass using a dye Mitotracker Green which stains mitochondrion independent of mitochondrial membrane potential. We found that XCT-790 decreased mitochondrial masses in both cell lines in dose dependent manners (Fig. 2b). Additionally, we measured and found that mitochondrial DNA contents were reduced in time-dependent manners (Fig. 2c) coinciding with the reduction of ERRα and PGC-1α protein levels.

3.3. Effects of XCT-790 on mitochondrial membrane potential

In addition to suppressing mitochondrial mass, we studied if mitochondrial membrane potential ($\Delta\Psi_m$) was affected by XCT-790 treatment. We measured the changes in $\Delta\Psi_m$ with a fluorescent dye JC-1 that gives a red fluorescence when $\Delta\Psi_m$ is high and green fluorescence when $\Delta\Psi_m$ is low. When cells were treated with XCT-790 for 24 h, we found that the percentage of cells with red fluorescence increased in both HepG2 and R-HepG2 cells in dose-dependent manners (Fig. 3a). But when cells were treated with XCT-790 for 48 or 72 h, time-dependent decreases of red/green fluorescence ratio were observed in HepG2 and R-HepG2 (Fig. 3b), suggesting that the mitochondrial function was dysregulated.

3.4. Effects of XCT-790 on ROS level and caspases activities

Mitochondrial dysfunction results in a variety of deleterious outcomes including generation of reactive oxygen species (ROS) [20]. Accumulation of ROS can lead to cell death through activation of caspases [21]. We therefore examined the generation of ROS using flow cytometry with 2, 7-dichlorodihydrofluorescin diacetate (DCFH-DA) dye. We found that XCT-790 increased ROS levels in both HepG2 and R-HepG2 cells in dose- (Fig. 4a) and time-dependent manners (Fig. 4b). Furthermore, XCT-790 increased caspase 3/7, 8, and 9 activities (Fig. 4c–e). Notably, we also found that an anti-oxidative compound MnTBAP, which is a cell-permeable superoxide

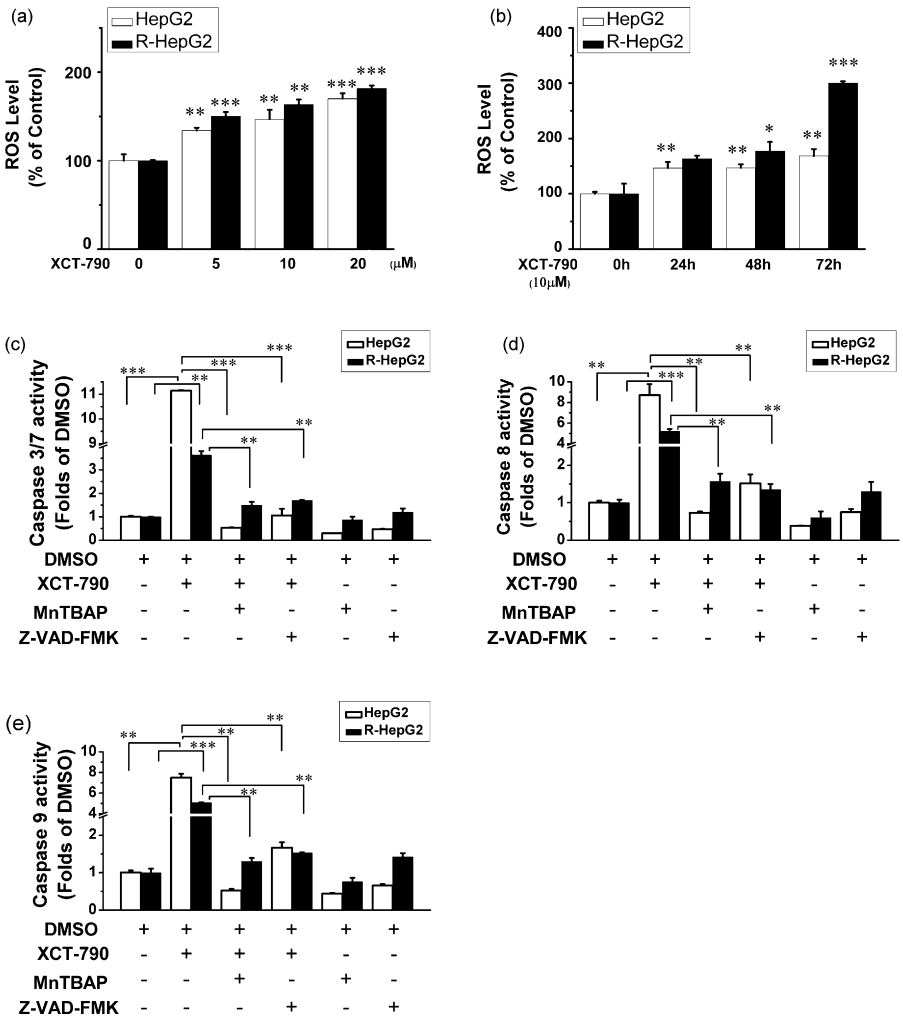

Fig. 4. Effects of XCT-790 on ROS level and caspases activities. (a) ROS levels were determined by measuring the fluorescence of DCF. HepG2 and R-HepG2 cells were treated with DMSO or XCT-790 at the concentrations indicated for 24 h. The relative levels were presented as the percentage of DMSO control. (b) ROS levels in HepG2 and R-HepG2 cells were treated with DMSO or 10 μM XCT-790 for the time indicated were measured as in (a). (c–e) Caspase 3/7(c), 8(d) and 9(e) activities in the presence of DMSO or 10 μM XCT-790 with or without 200 μM MnTBAP/40 μM Z-VAD-FMK for 48 h were determined in HepG2 and R-HepG2. Relative caspase 3/7, 8 and 9 activities were presented as the fold of DMSO control. Values are shown as mean ± SD of three independent experiments. Asterisks indicate significant differences ($^{*}P < 0.05$, $^{**}P < 0.01$, $^{***}P < 0.001$).

dismutase (SOD) mimetic and peroxynitrite scavenger [22], blocked the caspases activities increased by XCT-790 treatment (Fig. 4c–e).

3.5. Effects of XCT-790 on cell death

Next, we confirmed if the XCT-790 induced ROS and caspases activities would lead to cell death in HepG2 and R-HepG2. Cells treated with XCT-790 were analyzed for the presence of early apoptotic events such as PS externalization and loss of membrane integrity upon Annexin V-PE and 7-AAD staining. We found that XCT-790 induced apoptosis in the two cell lines with HepG2 being more sensitive compared to R-HepG2 and that ROS scavenger MnTBAP prevented cells from XCT-790-induced cell death (Fig. 5a). In addition, we found that a pan-caspase inhibitor Z-VAD-FMK blocked the XCT-790-induced caspases activities (Fig. 4c–e) and cell death (Fig. 5a), strongly suggesting that the ROS-mediated activation of caspases is responsible for the apoptosis induced by XCT-790. Importantly, XCT-790 synergized with taxol but not doxorubicin to promote cell death in R-HepG2 (Fig. 5b and c), suggesting that XCT-790 treatment may be selectively combined with current anticancer agents to maximize therapeutic effect.

4. Discussion

Doxorubicin, paclitaxel, and cisplatin, representing different classes of chemotherapeutics, have been widely used for the treatments of various types of cancer. The initial efficacies for these chemotherapeutics vary with certain patients having more sensitive while others more resistant tumors. The mechanisms of multi-drug resistance have been at least attributed to the aberrant expression or activities of ATP-binding cassette transporters [13,14]. Therefore, novel chemotherapeutics that are not affected by these transporters may have important therapeutic values.

ERRα is primarily thought to regulate energy metabolism [2]. Nonetheless, over-expression of ERRα has been associated with poor clinical outcome in breast cancer patients [3,7]. It is therefore reasonable to speculate that suppressing ERRα activity pharmacologically would be a novel way to suppress tumor growth. In this study, we presented evidences that an ERRα inverse agonist XCT-790 would be able to overcome MDR in cancer cells with different levels of drug resistance. Importantly, XCT-790 was effective in suppressing the growth of R-HepG2 cells which displayed strong doxorubicin resistance.

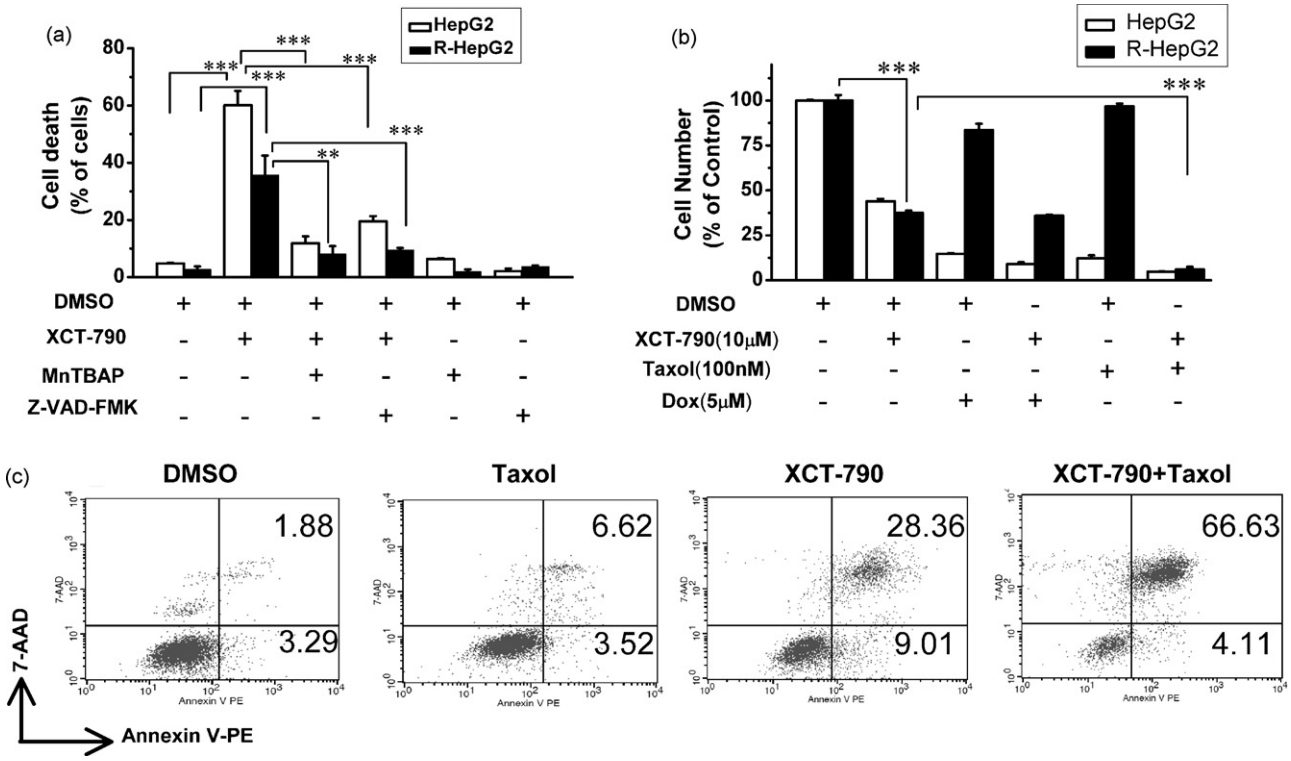

Fig. 5. Effects of XCT-790 on apoptosis. (a) HepG2 and R-HepG2 cells were treated with DMSO or 10 μM XCT-790 with or without 200 μM MnTBAP/40 μM Z-VAD-FMK for 48 h. Cells were then incubated with Annexin V-PE and 7-AAD and subjected to flow cytometric analysis. The percentage of dead cells (including early apoptosis and end stage apoptosis) are shown. (b) HepG2 and R-HepG2 cells were treated with DMSO or 10 μM XCT-790 with or without 5 μM Dox/100 nM Taxol for 48 h and cell viabilities were measured. (c) R-HepG2 cells were treated with DMSO or 10 μM XCT-790 with or without 100 nM Taxol for 48 h. Then the Cells were incubated with Annexin V-PE and 7-AAD and subjected to flow cytometric analysis. The numbers at the corners represent the percentage of cells in the corresponding quadrants. Values are shown as mean ± SD of three independent experiments. Asterisks indicate significant differences ($^{*}P < 0.05$, $^{**}P < 0.01$, $^{***}P < 0.001$).

We demonstrated that the mechanism of XCT-790-induced apoptosis involved the generation of ROS due to mitochondrial dysfunction. At an early stage upon XCT-790 treatment, $\Delta\Psi_m$ was elevated in cells in which the activity of ERRα was suppressed. This elevated $\Delta\Psi_m$ would be expected to generate more ATP per mitochondrion in order to compensate for the lost of ATP production capacity due to an overall lower amount of mitochondria resulting from the reductions of ERRα and PGC-1α expressions. The hyperactivated $\Delta\Psi_m$ may then lead to an over-production of ROS as more electrons are passed through the electron transport chain. This initial elevation of ROS may lead to damages to the mitochondria and eventually resulting in depolarization and a reduction of $\Delta\Psi_m$. Consistently, XCT-790 dose- and time-dependently increased ROS levels and activated a caspase-mediated apoptotic pathway.

R-HepG2 cells express MDR1 at high levels and display MDR to a variety of functionally and structurally unrelated chemotherapeutic agents [15]. Coincidentally, R-HepG2 cells have higher mitochondrial mass, $\Delta\Psi_m$ and ROS levels compared to HepG2 (data not shown). The mRNA expression levels of anti-oxidative enzymes glutathione peroxidase (GPx), manganese superoxide dismutase (MnSOD), copper superoxide dismutase (CuSOD), and mitochondrial uncoupling protein 2 (UCP2) are reduced in R-HepG2 compared to HepG2 (data not shown). These changes may be the reason behind the higher levels of ROS and $\Delta\Psi_m$ observed in R-HepG2 compared to HepG2. These data suggest that R-HepG2 cells have adopted to proliferate under a high basal level of ROS. This adaptation may help R-HepG2 cells survive through the increase in ROS mediated by certain types of chemotherapeutics like doxorubicin. Correspondingly, the increases in caspases activities and extent of apoptosis were lower in R-HepG2 than HepG2 (Figs. 4c–e and 5a) despite a higher level of ROS induced by XCT-790 (Fig. 4b). Therefore, the reduction of mitochondrial mass may also be in part responsible for the growth suppression mediated by XCT-790.

Although further investigation into the specific mechanism of how XCT-790 overcomes MDR is warranted, our preliminary results suggest that developing novel chemotherapeutics based on targeting ERRα to suppress cancer growth may be a viable strategy. Particularly, XCT-790 selectively synergized with taxol but not doxorubicin to induce apoptosis in R-HepG2 cells (Fig. 5b). Doxorubicin induces ROS through inflicting DNA damages whereas taxol alters microtubule stability without known ROS inductive effect. Mechanistically, taxol may complement the ROS mediated caspase activation induced by XCT-790 better than doxorubicin. These preliminary data also suggest that additional exploration of different combinations of chemotherapeutics with XCT-790 may pave ways for future pre-clinical development.

Conflict of interest

All authors disclose no financial and personal relationships with other people or organizations that could inappropriately influence (bias) this work.

Acknowledgements

The research is supported by grants from the National Natural Science Foundation of China #30672463, the National Basic Research Program of China (973-Program) #2006CB50390, and the Knowledge Innovation Program of the Chinese Academy of Sciences # KSCX2-YW-R-085.

References

[1] B. Horard, J.M. Vanacker, Estrogen receptor-related receptors: orphan receptors desperately seeking a ligand, J. Mol. Endocrinol. 31 (3) (2003) 349–357.

[2] V. Giguere, Transcriptional control of energy homeostasis by the estrogen-related receptors, Endocr. Rev. 29 (6) (2008) 677–696.

[3] T. Suzuki, Y. Miki, T. Moriya, N. Shimada, T. Ishida, H. Hirakawa, N. Ohuchi, H. Sasano, Estrogen-related receptor alpha in human breast carcinoma as a potent prognostic factor, Cancer Res. 64 (13) (2004) 4670–4676.

[4] P. Sun, J. Sehouli, C. Denkert, A. Mustea, D. Konsgen, I. Koch, L. Wei, W. Lichtenegger, Expression of estrogen receptor-related receptors, a subfamily of orphan nuclear receptors, as new tumor biomarkers in ovarian cancer cells, J. Mol. Med. (Berlin, Germany) 83 (6) (2005) 457–467.

[5] C.P. Cheung, S. Yu, K.B. Wong, L.W. Chan, F.M. Lai, X. Wang, M. Suetsugi, S. Chen, F.L. Chan, Expression and functional study of estrogen receptor-related receptors in human prostatic cells and tissues, J. Clin. Endocrinol. Metab. 90 (3) (2005) 1830–1844.

[6] A. Cavallini, M. Notarnicola, R. Giannini, S. Montemurro, D. Lorusso, A. Visconti, F. Minervini, M.G. Caruso, Oestrogen receptor-related receptor alpha (ERRalpha) and oestrogen receptors (ERalpha and ERbeta) exhibit different gene expression in human colorectal tumour progression, Eur. J. Cancer 41 (10) (2005) 1487–1494.

[7] E.A. Ariazi, G.M. Clark, J.E. Mertz, Estrogen-related receptor alpha and estrogen-related receptor gamma associate with unfavorable and favorable biomarkers, respectively, in human breast cancer, Cancer Res. 62 (22) (2002) 6510–6518.

[8] D.P.M.R.A. Stein, Estrogen-related receptor as a therapeutic target in cancer, Endocr. Related Cancer 13 (sup1) (2006) S25–32.

[9] R.A. Stein, C.-y. Chang, D.A. Kazmin, J. Way, T. Schroeder, M. Wergin, M.W. Dewhirst, D.P. McDonnell, Estrogen-Related, Receptor alpha is critical for the growth of estrogen receptor-negative breast cancer, Cancer Res. 68 (21) (2008) 8805–8812.

[10] B.B. Busch, W.C. Stevens, R. Martin, P. Ordentlich, S. Zhou, D.W. Sapp, R.A. Horlick, R. Mohan, Identification of a selective inverse agonist for the orphan nuclear receptor estrogen-related receptor alpha, J. Med. Chem. 47 (23) (2004) 5593–5596.

[11] O. Lanvin, S. Bianco, N. Kersual, D. Chalbos, J.-M. Vanacker, Potentiation of ICI182,780 (Fulvestrant)-induced estrogen receptor-alpha degradation by the estrogen receptor-related receptor-alpha inverse agonist XCT790, J. Biol. Chem. 282 (39) (2007) 28328–28334.

[12] V. Ling, Multidrug resistance: molecular mechanisms and clinical relevance, Cancer Chemother. Pharmacol. 40 (Suppl) (1997) S3–8.

[13] M.M. Gottesman, I. Pastan, Biochemistry of multidrug resistance mediated by the multidrug transporter, Annu. Rev. Biochem. 62 (1993) 385–427.

[14] O. Fardel, V. Lecureur, A. Guillouzo, The P-glycoprotein multidrug transporter, Gen. Pharmacol. 27 (8) (1996) 1283–1291.

[15] Y.C. Li, K.P. Fung, T.T. Kwok, C.Y. Lee, Y.K. Suen, S.K. Kong, Mitochondrial targeting drug lonidamine triggered apoptosis in doxorubicin-resistant HepG2 cells, Life Sci. 71 (23) (2002) 2729–2740.

[16] M. Sundaresan, Z.X. Yu, V.J. Ferrans, K. Irani, T. Finkel, Requirement for generation of H_2O_2 for platelet-derived growth factor signal transduction, Science 270 (5234) (1995) 296–299.

[17] J.S. Koo, W.C. Choi, Y.H. Rhee, H.J. Lee, E.O. Lee, K.S. Ahn, H.S. Bae, J.M. Kang, S.U. Choi, M.O. Kim, J. Lu, S.H. Kim, Quinoline derivative KB3-1 potentiates paclitaxel induced cytotoxicity and cycle arrest via multidrug resistance reversal in MES-SA/DX5 cancer cells, Life Sci. 83 (21–22) (2008) 700–708.

[18] J.M. Huss, I.P. Torra, B. Staels, V. Giguere, D.P. Kelly, Estrogen-related receptor {alpha} directs peroxisome proliferator-activated receptor alpha signaling in the transcriptional control of energy metabolism in cardiac and skeletal muscle, Mol. Cell. Biol. 24 (20) (2004) 9079–9091.

[19] S.N. Schreiber, R. Emter, M.B. Hock, D. Knutti, J. Cardenas, M. Podvinec, E.J. Oakeley, A. Kralli, The estrogen-related receptor alpha (ERR alpha) functions in PPAR gamma coactivator 1 alpha (PGC-1 alpha)-induced mitochondrial biogenesis, PNAS 101 (17) (2004) 6472–6477.

[20] A.A. Starkov, The role of mitochondria in reactive oxygen species metabolism and signaling, Ann. N Y Acad. Sci. 1147 (2008) 37–52.

[21] C. Fleury, B. Mignotte, J.-L. Vayssière, Mitochondrial reactive oxygen species in cell death signaling, Biochim. 84 (2–3) (2002) 131–141.

[22] H. Kadowaki, H. Nishitoh, F. Urano, C. Sadamitsu, A. Matsuzawa, K. Takeda, H. Masutani, J. Yodoi, Y. Urano, T. Nagano, H. Ichijo, Amyloid beta induces neuronal cell death through ROS-mediated ASK1 activation, Cell Death Differ 12 (1) (2005) 19–24.